Replacement of microglia by brain-engrafted macrophages provide protection against concussive injury

Xi Feng[1,2], Elma S. Frias[1,2], Maria S. Paladini[1,2], David Chen[1,2,3], Zoe Boosalis[1,2],McKenna Becker[1,2], Sonali Gupta[1,2], Sharon Liu[3], Nalin Gupta[3,6,7] and Susanna Rosi[1,2,3,4,5*]

[1] Brain and Spinal Injury Center

[2] Department of Physical Therapy and Rehabilitation Science

[3] Department of Neurological Surgery

[4] Weill Institute for Neuroscience

[5] Kavli Institute of Fundamental Neuroscience

[6] Brain Tumor Research Center

[7] Department of Pediatrics

University of California San Francisco

* Corresponding Author

Susanna Rosi Ph.D.: Susanna.Rosi@ucsf.edu

1001 Potrero Ave, Building 1, Room 101, Zuckerberg San Francisco General Hospital
Department of Physical Therapy and Rehabilitation Science, University of California, San Francisco, San Francisco, CA 94110

Running Title: monocyte-derived macrophages protect against brain injury

Keywords: microglia, brain engrafted macrophages, cognition, brain irradiation, CSF-1R inhibitor

Abstract

Brain resident microglia have a distinct origin compared to macrophages in other organs. Under physiological conditions, microglia are maintained by self-renewal from the local pool, independent of hematopoietic progenitors. Pharmacological depletion of microglia during therapeutic whole-brain irradiation prevents synaptic loss and long-term recognition memory deficits. Here we demonstrate that after concurrent therapeutic whole-brain irradiation and microglia depletion, macrophages originating from circulating monocytes engraft into the brain and replace the microglia pool. Comparisons of transcriptomes reveal that brain-engrafted macrophages have an intermediate phenotype which resembles both monocytes and embryonic microglia. In response to a secondary concussive brain injury, brain-engrafted macrophages display reduced phagocytic activity for synaptic compartments compared to that of microglia from normal brain. Notably, mice bearing engrafted macrophages are spared from concussive injury-induced memory loss. Taken together, our data demonstrate that replacement of microglia by brain-engrafted macrophages provides protection against concussive brain injury-induced memory deficits.

Brain resident microglia are the innate immune cells of the central nervous system (CNS). Arising from the yolk sac during embryonic development, microglia actively survey the environment to maintain normal brain functions (*1, 2*). Under physiological conditions, microglia populations are maintained solely by self-renewal from the local pool (*3*). Following brain injury and other pathological conditions, microglia become activated and play a central role in the clearance of cellular debris. However, if not controlled this process can result in aberrant synaptic engulfment (*4-7*). Temporary depletion of microglia can be achieved by using pharmacologic inhibitors of the colony-stimulating factor 1 receptor (CSF-1R) (*8*). In the normal brain, treatment with CSF-1R inhibitors (CSF-1Ri) can deplete up to 99% of microglia without causing detectable changes to cognitive functions (*8, 9*). Full repopulation occurs within 14 days of inhibitor withdrawal, and the repopulated microglia are morphologically and functionally identical to the microglia in naïve brains (*9*). Microglia depletion and repopulation by local progenitors has been shown to be beneficial for disease- ,injury- , and age-associated neuropathological and behavioral conditions(*10-15*).

Whole-brain radiotherapy (WBRT), delivered in multiple fractions, is routinely used to treat patients with brain tumors. While it is effective in intracranial tumor control, WBRT leads to deterioration of cognitive function and quality of life in patients(*16-18*). Depletion of microglia during or shortly after whole-brain irradiation in animal models can prevent long term radiation-induced loss of dendritic spines in hippocampal neurons and memory impairments(*12-14*)(and **Supplementary Figure 1**). These results demonstrate the critical role that microglia play in inducing synaptic abnormalities and consequently, cognitive deficits after brain irradiation. However, the cell-of-origin and functions of repopulated “microglia” after microglia depletion and WBRT are unknown. In the current study, we demonstrate the origin and functionality of repopulated microglia-like cells after concurrent microglia depletion and WBRT.

The fractalkine receptor CX3CR1 is expressed in both microglia and peripheral monocytes (*19*), while chemokine receptor CCR2 is mainly expressed in monocytes (*20*). In the Cx3cr1$^{GFP/+}$Ccr2$^{RFP/+}$ reporter mice, the expression patterns of GFP and RFP can be used to distinguish microglia (GFP+RFP-) from monocytes (GFP+RFP+) (*20*). To investigate the origin of the cells that repopulate after concurrent microglia depletion and WBRT we generated bone marrow chimeras with head-protected irradiation using fluorescent labeled bone marrow from Cx3cr1$^{GFP/+}$Ccr2$^{RFP/+}$ donor mice (**Figure 1a**). This approach allowed partial replacement of bone marrow cells without changing the permeability of the blood-brain-barrier (*2, 21, 22*). At six weeks after bone marrow transplantation about two thirds of peripheral monocytes were replaced by transplanted cells with fluorescent labels (**Figure 1b**). Bone marrow chimera animals were then treated with WBRT and CSF-1R inhibitor. Next we compared the compositions of myeloid cells in the brain after CSF-1R inhibitor-mediated depletion and repopulation. Flow cytometry analyses performed 33 days after WBRT revealed that microglia depletion and repopulation alone (Sham + CSF-1Ri) only resulted in limited accumulation of transplanted cells in the brain (**Figure 1c, BMT only**). However, in mice that received WBRT and CSF-1Ri, two thirds of the microglia were replaced by Cx3cr1-GFP labeled cells (**Figure 1c, BMT +fWBI**). These results demonstrate that peripheral monocyte-derived BEMs are the major component of the CNS myeloid cell pool after WBRT and microglia depletion. Importantly, radiation-induced differentially expressed genes in stress/radiation response, cell cycle regulation and DNA repair pathways were only found in the WBRT treated but not in CSF-1Ri or WBRT+CSF-1Ri treated brains (**Supplementary Figure 2**).

We next assessed the transcriptomic signature of the BEMs after microglia depletion and WBRT by comparing our RNAseq dataset with a previous report by Lavin and Winter *et al* (*23*). To minimize false discovery and noise signals, we examined 1201 genes from this published dataset with a fold change greater than 1.50 or smaller than 0.667 for down-regulated genes

($p<0.05$, monocyte compared to naïve microglia), and found that 1066 genes were expressed in our samples (**Table S1**). Strikingly, the hierarchical clustering of 525 monocyte- and 541 microglia-signature genes revealed that the expression profile of monocyte-derived BEMs (WBRT + CSF-1Ri) does not cluster with naïve (Sham + Control diet), irradiated (WBRT + Control diet) or repopulated (Sham + CSF-1Ri) microglia (**Figure 1d**). A similarity matrix analysis using this microglia/monocyte signature gene list revealed that the expression pattern in BEMs is different from naïve, irradiated and repopulated microglia (**Figure 1e**). We counted genes in each group that expressed in the same trends as microglia or monocyte signature genes from the Lavin data set to determine the similarity scores to these two cell populations. Naïve, irradiated and repopulated microglia had 60%, 57% and 51% (718, 685 and 612) genes expressed in the same trends as microglia signature genes, respectively, with minimum similarity (2-3%) to monocyte signature genes; while BEMs expressed both microglia (28%, 331 genes) and monocyte signature genes (32%, 386 genes) (**Figure 1f**). These results validate that after concurrent microglia depletion and WBRT, BEMs originate from blood monocytes (see **Supplementary Figure 3** for qPCR validation of microglia vs monocyte markers).

To determine whether BEMs are present long-term in the brain, we monitored this cellular population six months after WBRT. To eliminate the limitation of using bone marrow obtained from the Cx3cr1$^{+/GFP}$Ccr2$^{+/RFP}$ knock-in reporter mouse strain, we used an actin-GFP transgenic line as bone marrow donors and generated chimeras using the same body-only irradiation protocol (**Figure 2 a**). Six weeks later, mice were treated with CSF-1R inhibitor and WBRT and then used to trace BEMs at varies time points (**Figure 2 a**). Whole coronal sections at the level of the dorsal hippocampus were stained with Iba1 and imaged to quantify total Iba1+ and GFP+ cells (**Supplementary Figure 4 a**). We found that all GFP+ cells in the brain were also Iba1+, suggesting that BEMs were indeed derived from the periphery. In addition, the morphology of Iba1+GFP+ BEMs were analyzed and compared to Iba1+GFP- microglia (**Figure**

2 b and d). We found that round-shaped Iba1+GFP+ BEM cells entered the brain starting from 7 days after WBRT, and started to obtain more processes that resembled microglia morphology (**Figure 2 b**). However, Sholl analysis demonstrated that the morphology of BEMs remained stable from 33 days after WBRT and never reached the structural complexity of microglia (**Figure 2c, Supplementary Figure 5**). We found that 40 – 90% of Iba1+ cells are also GFP+ at 14 days after WBRT. This ratio remained at high levels at one, three and six months after WBRT (**Figure 2 e**). Interestingly, although the Iba1+ and Iba1+GFP+ cell numbers were not fully recovered at 14 days after WBRT, the microglia replacement ratio was similar to the level of later time points (**Figure 2 e and Supplementary Figure 4 b and c**), suggesting a non-competitive manner of brain parenchyma occupancy by microglia and BEMs. These data demonstrate that BEMs enter the brain shortly after WBRT, adapt to a microglia-like morphology and maintain a stable population.

We have previously reported that a single mild concussive Closed Head Injury (CHI) can induce memory deficits in mice(*24, 25*). To investigate the function of BEMs after they replaced microglia, a CHI was given to mice 30 days after CSF-1R inhibitor treatment and WBRT; microglia/BEMs morphology and phagocytic activities were measured following recognition memory test by NOR (**Fig 3 a**). By FACS analysis at 24 days post injury, we found that phagocytosis activity increased (p=0.0419) after CHI in microglia but not in BEMs (**Figure 3 b**). Quantification of immunofluorescent staining of Iba-1/PSD-95 co-localization revealed a trend of increased engulfment towards pre-stained synaptosomes by microglia, but not by BEMs (**Fig 3 c and d**). In addition, Sholl analysis demonstrated that the structural complexity of microglia decreased, while the morphology of BEMs remained unchanged after CHI (**Figure 3 e**). Furthermore, at 20 days after injury, CHI-induced recognition memory deficits were spared in mice whose microglia were replaced by BEMs (**Figure 3 f**). These results demonstrate that unlike resident microglia, which transition to a less ramified morphology and exhibit increased

phagocytic activity towards injected synaptosomes, BEMs remain unchanged in both morphology and phagocytic activity in response to CHI. More importantly, our data suggest that replacement of microglia by BEMs can protect against CHI-induced memory loss.

Here we demonstrate that peripheral monocytes contribute largely to repopulated microglia-like cells after concurrent microglia depletion and WBRT. After entering the brain, BEMs gradually gain a microglia-like morphology but never reach the structural complexity of microglia. BEMs persist in the brain and express both microglia and monocyte signature genes. More importantly, unlike microglia which respond to CHI by upregulating their phagocytic capacity and undergo structural changes toward a more amoeboid-like morphology, BEMs remain unchanged in both regards. As a result, BEM-bearing animals are spared from CHI-induced memory deficits. Our results provide evidence for the involvement of microglia as a direct cause of memory deficits after concussive injury, which can be prevented by replacement of microglia by BEMs.

Acknowledgements (optional)

This work was funded by grants from the National Institutes of Health no. R01CA133216 and R01CA213441 (S.R.), R01AG056770 (S.R).

Author contributions

X.F. conceptualized the study, designed and performed the experiments, analyzed the data and wrote the manuscript. E.F. performed experiments, analyzed the data, drew the graphic abstract and wrote the manuscript. M.P performed experiments, analyzed the data and revised the manuscript. D.C. assisted in the in vivo phagocytosis assay and data analysis. Z.B. helped with the in vivo phagocytosis assay imaging and data analysis. M.B. assisted in the Sholl analysis of microglia and BEMs. S.G analyzed the long-term dendritic spine counts data. S.L. provided assistance in experiments related to WBRT and BM chimeras. N.G. provided critical inputs to the study and revised the manuscript. S.R. conceptualized and supervised the study and revised the manuscript. All authors approved the final version of the manuscript.

Competing interests

The authors declare no competing interests.

Reference

1. F. Alliot, I. Godin, B. Pessac, Microglia derive from progenitors, originating from the yolk sac, and which proliferate in the brain. *Developmental Brain Research* **117**, 145-152 (1999); published online Epub1999/11/18/ (https://doi.org/10.1016/S0165-3806(99)00113-3).
2. F. Ginhoux, M. Greter, M. Leboeuf, S. Nandi, P. See, S. Gokhan, M. F. Mehler, S. J. Conway, L. G. Ng, E. R. Stanley, I. M. Samokhvalov, M. Merad, Fate Mapping Analysis Reveals That Adult Microglia Derive from Primitive Macrophages. *Science* **330**, 841 (2010).
3. B. Ajami, J. L. Bennett, C. Krieger, W. Tetzlaff, F. M. V. Rossi, Local self-renewal can sustain CNS microglia maintenance and function throughout adult life. *Nature Neuroscience* **10**, 1538 (2007)
4. M. Prinz, J. Priller, S. S. Sisodia, R. M. Ransohoff, Heterogeneity of CNS myeloid cells and their roles in neurodegeneration. *Nat Neurosci* **14**, 1227-1235 (2011); published online EpubSep 27 (10.1038/nn.2923).
5. K. Saijo, C. K. Glass, Microglial cell origin and phenotypes in health and disease. *Nat Rev Immunol* **11**, 775-787 (2011); published online EpubNov (10.1038/nri3086).
6. S. Hong, L. Dissing-Olesen, B. Stevens, New insights on the role of microglia in synaptic pruning in health and disease. *Current opinion in neurobiology* **36**, 128-134 (2015); published online EpubDec 30 (10.1016/j.conb.2015.12.004).
7. S. Hong, B. Stevens, Microglia: Phagocytosing to Clear, Sculpt, and Eliminate. *Developmental Cell* **38**, 126-128 (2016); published online Epub2016/07/25/ (https://doi.org/10.1016/j.devcel.2016.07.006).
8. M. R. Elmore, A. R. Najafi, M. A. Koike, N. N. Dagher, E. E. Spangenberg, R. A. Rice, M. Kitazawa, B. Matusow, H. Nguyen, B. L. West, K. N. Green, Colony-stimulating factor 1 receptor signaling is necessary for microglia viability, unmasking a microglia progenitor cell in the adult brain. *Neuron* **82**, 380-397 (2014); published online EpubApr 16 (10.1016/j.neuron.2014.02.040).

9. M. R. Elmore, R. J. Lee, B. L. West, K. N. Green, Characterizing newly repopulated microglia in the adult mouse: impacts on animal behavior, cell morphology, and neuroinflammation. *PLoS One* **10**, e0122912 (2015)10.1371/journal.pone.0122912).
10. N. N. Dagher, A. R. Najafi, K. M. Kayala, M. R. Elmore, T. E. White, R. Medeiros, B. L. West, K. N. Green, Colony-stimulating factor 1 receptor inhibition prevents microglial plaque association and improves cognition in 3xTg-AD mice. *Journal of neuroinflammation* **12**, 139 (2015)10.1186/s12974-015-0366-9).
11. E. E. Spangenberg, R. J. Lee, A. R. Najafi, R. A. Rice, M. R. P. Elmore, M. Blurton-Jones, B. L. West, K. N. Green, Eliminating microglia in Alzheimer's mice prevents neuronal loss without modulating amyloid-β pathology. *Brain*, (2016); published online Epub2016-02-26 00:00:00 (10.1093/brain/aww016).
12. M. M. Acharya, K. N. Green, B. D. Allen, A. R. Najafi, A. Syage, H. Minasyan, M. T. Le, T. Kawashita, E. Giedzinski, V. K. Parihar, B. L. West, J. E. Baulch, C. L. Limoli, Elimination of microglia improves cognitive function following cranial irradiation. *Scientific reports* **6**, 31545 (2016); published online EpubAug 12 (10.1038/srep31545).
13. X. Feng, T. D. Jopson, M. S. Paladini, S. Liu, B. L. West, N. Gupta, S. Rosi, Colony-stimulating factor 1 receptor blockade prevents fractionated whole-brain irradiation-induced memory deficits. *Journal of neuroinflammation* **13**, 215 (2016)10.1186/s12974-016-0671-y).
14. X. Feng, S. Liu, D. Chen, S. Rosi, N. Gupta, Rescue of cognitive function following fractionated brain irradiation in a novel preclinical glioma model. *eLife* **7**, e38865 (2018); published online Epub2018/11/13 (10.7554/eLife.38865).
15. K. Krukowski, X. Feng, M. S. Paladini, A. Chou, K. Sacramento, K. Grue, L. K. Riparip, T. Jones, M. Campbell-Beachler, G. Nelson, S. Rosi, Temporary microglia-depletion after cosmic radiation modifies phagocytic activity and prevents cognitive deficits. *Scientific reports* **8**, 7857 (2018); published online EpubMay 18 (10.1038/s41598-018-26039-7).
16. R. Stupp, W. P. Mason, M. J. van den Bent, M. Weller, B. Fisher, M. J. B. Taphoorn, K. Belanger, A. A. Brandes, C. Marosi, U. Bogdahn, J. Curschmann, R. C. Janzer, S. K. Ludwin, T. Gorlia, A. Allgeier, D. Lacombe, J. G. Cairncross, E. Eisenhauer, R. O. Mirimanoff, Radiotherapy plus Concomitant and Adjuvant Temozolomide for Glioblastoma. *New England Journal of Medicine* **352**, 987-996 (2005); published online Epub2005/03/10 (10.1056/NEJMoa043330).
17. D. Greene-Schloesser, M. E. Robbins, Radiation-induced cognitive impairment--from bench to bedside. *Neuro Oncol* **14 Suppl 4**, iv37-44 (2012); published online EpubSep (10.1093/neuonc/nos196).
18. C. Shinohara, G. T. Gobbel, K. R. Lamborn, E. Tada, J. R. Fike, Apoptosis in the Subependyma of Young Adult Rats after Single and Fractionated Doses of X-Rays. *Cancer Research* **57**, 2694-2702 (1997).
19. S. Jung, J. Aliberti, P. Graemmel, M. J. Sunshine, G. W. Kreutzberg, A. Sher, D. R. Littman, Analysis of Fractalkine Receptor CX₃CR1 Function by Targeted Deletion and Green Fluorescent Protein Reporter Gene Insertion. *Molecular and cellular biology* **20**, 4106 (2000)10.1128/MCB.20.11.4106-4114.2000).
20. N. Saederup, A. E. Cardona, K. Croft, M. Mizutani, A. C. Cotleur, C.-L. Tsou, R. M. Ransohoff, I. F. Charo, Selective Chemokine Receptor Usage by Central Nervous System Myeloid Cells in CCR2-Red Fluorescent Protein Knock-In Mice. *PLoS ONE* **5**, e13693 (2010)10.1371/journal.pone.0013693).
21. A. Mildner, H. Schmidt, M. Nitsche, D. Merkler, U.-K. Hanisch, M. Mack, M. Heikenwalder, W. Bruck, J. Priller, M. Prinz, Microglia in the adult brain arise from Ly-6ChiCCR2+ monocytes only under defined host conditions. *Nat Neurosci* **10**, 1544-1553 (2007)

22. J. Priller, A. Flügel, T. Wehner, M. Boentert, C. A. Haas, M. Prinz, F. Fernández-Klett, K. Prass, I. Bechmann, B. A. de Boer, M. Frotscher, G. W. Kreutzberg, D. A. Persons, U. Dirnagl, Targeting gene-modified hematopoietic cells to the central nervous system: Use of green fluorescent protein uncovers microglial engraftment. *Nature Medicine* **7**, 1356-1361 (2001); published online Epub2001/12/01 (10.1038/nm1201-1356).
23. Y. Lavin, D. Winter, R. Blecher-Gonen, E. David, H. Keren-Shaul, M. Merad, S. Jung, I. Amit, Tissue-resident macrophage enhancer landscapes are shaped by the local microenvironment. *Cell* **159**, 1312-1326 (2014); published online EpubDec 4 (10.1016/j.cell.2014.11.018).
24. A. Chou, K. Krukowski, T. Jopson, P. J. Zhu, M. Costa-Mattioli, P. Walter, S. Rosi, Inhibition of the integrated stress response reverses cognitive deficits after traumatic brain injury. *Proceedings of the National Academy of Sciences* **114**, E6420 (2017)10.1073/pnas.1707661114).
25. K. Krukowski, A. Nolan, E. S. Frias, K. Grue, M. Becker, G. Ureta, L. Delgado, S. Bernales, V. S. Sohal, P. Walter, S. Rosi, Integrated Stress Response Inhibitor Reverses Sex-Dependent Behavioral and Cell-Specific Deficits after Mild Repetitive Head Trauma. *Journal of Neurotrauma* **37**, 1370-1380 (2019); published online Epub2020/06/01 (10.1089/neu.2019.6827).

Figure Legends

Figure 1: Repopulated cells after concurrent microglia depletion and WBRT are brain-engrafted macrophages originating from peripheral monocytes. **a** experimental design of head-protected bone marrow transplantation (BMT) followed by CSF-1Ri-mediated microglia depletion and WBRT. Lower panel shows fur colors before euthanasian for brain analysis. **b** representative FACS analysis gating strategy to analyze bone marrow chimera efficiency 6 weeks after BMT, about two thirds of the $CD11b^{+}Ly6C^{high}$ monocytes are replaced by $GFP^{+}RFP^{+}$ cells derived from donor bone marrow cells. **c** representative FACS analysis gating strategy and brain myeloid composition results. Upper panel shows FACS gating using CD45 and CD11b staining; microglia and microglia-like cells are defined by positive CD11b staining and low or intermediate CD45 levels. Lower panel shows scatter plots of GFP/RFP fluorescent levels of the $CD11b^{+}CD45^{low/intermediate}$ population in the brain, and a dot plot comparing percentages of peripheral myeloid cell derived microglia-like cells. Statistical analysis was performed using unpaired t-test, ***$p<0.001$. **d** hierarchically clustered heatmaps to compare microglia and monocyte signatures. A signature gene list was defined using a dataset published by Lavin and Winter et al, GSE63340. Defined list and expression details are in Table S1). **e** Similarity matrix comparisons using defined monocyte and microglia signature genes. **f** bar graph showing similarity scores to compare relative numbers of genes (in percentage of the defined list) that express in the same trends as monocytes or microglia based on the Lavin and Winter *et al* dataset.

Figure 2: BEMs gradually adapt to microglia-like morphology and persist in the brain. **a,** schematic of experimental design for long-term assessment of BEMs. **b,** representative images of microglia/BEMs counting, scale bar = 20 µm. **c**, Sholl analysis results showing numbers of intersections at different distances to cell center, BEMs at 7, 14, 33, 90 and 180 days after WBRT were compared to naïve microglia age-matched to 90 days after WBRT., representative

images showing differential Iba1 and GFP expressing bprofiles of microglia (Iba1+ GFP-) and BEMs (Iba1+ GFP+) in a BEM bearing brain at 33 days after WBRT. **e**, dot plot to show percentage of replacement of microglia by BEMs, each dot represent an individual mouse. n = 2 - 3. Statistical analyses were performed using unpaired t-test at each distance point (c) or time point (e). See Supplementary Figure 7 for detailed comparisons between microglia and BEMs at each time point.

Figure 3: Replacement of microglia by BEMs protects against concussive injury-induced memory deficits. **a**, schematic of experimental design for concussive injury, cognitive test and following analyses. **b**, dot plot to show the result of in vivo phagocytosis assay by FACS after injection of pre-stained synaptosomes, each dot represents value from an individual mouse, n = 4 -5. **c**, dot plot showing result of in vivo phagocytosis assay by IF imaging and quantification, each dot represents mean counts from an individual mouse, n = 3. **d**, representative images showing microglia and BEMs (arrows) phagocyting injected synaptosomes (green dots). **e**, Sholl analysis result showing numbers of intersections at different distances to the cell center, n = 5 - 6. **f**, dot plot showing NOR test result, each dot represent the performance of an individual mouse, n = 12. Statistical analyses were performed using two-way ANOVA with Tukey's multiple comparisons test (b and c) for each distance point (e) or unpaired t-test (f). *$p<0.05$, **$p<0.01$, ***$p<0.001$.

Figure 1

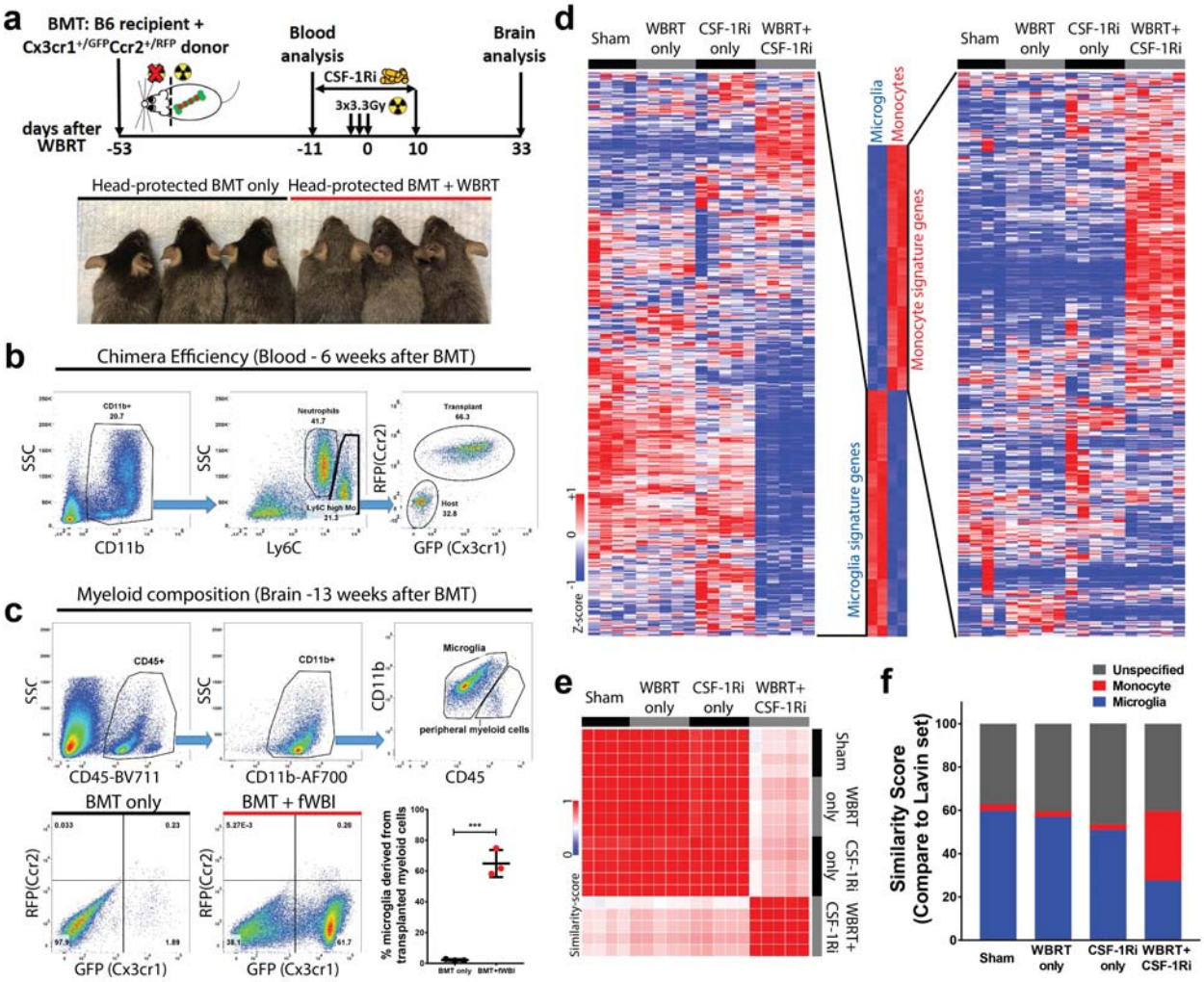
a
BMT: B6 recipient +
Cx3cr1+/GFPCcr2+/RFP donor
Blood analysis
Brain analysis
CSF-1Ri
3x3.3Gy
days after WBRT
-53
-11
0
10
33
Head-protected BMT only
Head-protected BMT + WBRT
b
Chimera Efficiency (Blood - 6 weeks after BMT)
CD11b+
Neutrophils
Transplant
Host
SSC
CD11b
Ly6C
RFP(Ccr2)
GFP (Cx3cr1)
c
Myeloid composition (Brain -13 weeks after BMT)
CD45+
CD11b+
Microglia
peripheral myeloid cells
CD45-BV711
CD11b-AF700
CD45
BMT only
BMT + fWBI
% microglia derived from transplanted myeloid cells
d
Sham
WBRT only
CSF-1Ri only
WBRT+ CSF-1Ri
Microglia
Monocytes
Monocyte signature genes
Microglia signature genes
Z-score
e
Similarity-score
f
Unspecified
Monocyte
Microglia
Similarity Score (Compare to Lavin set)

Figure 2

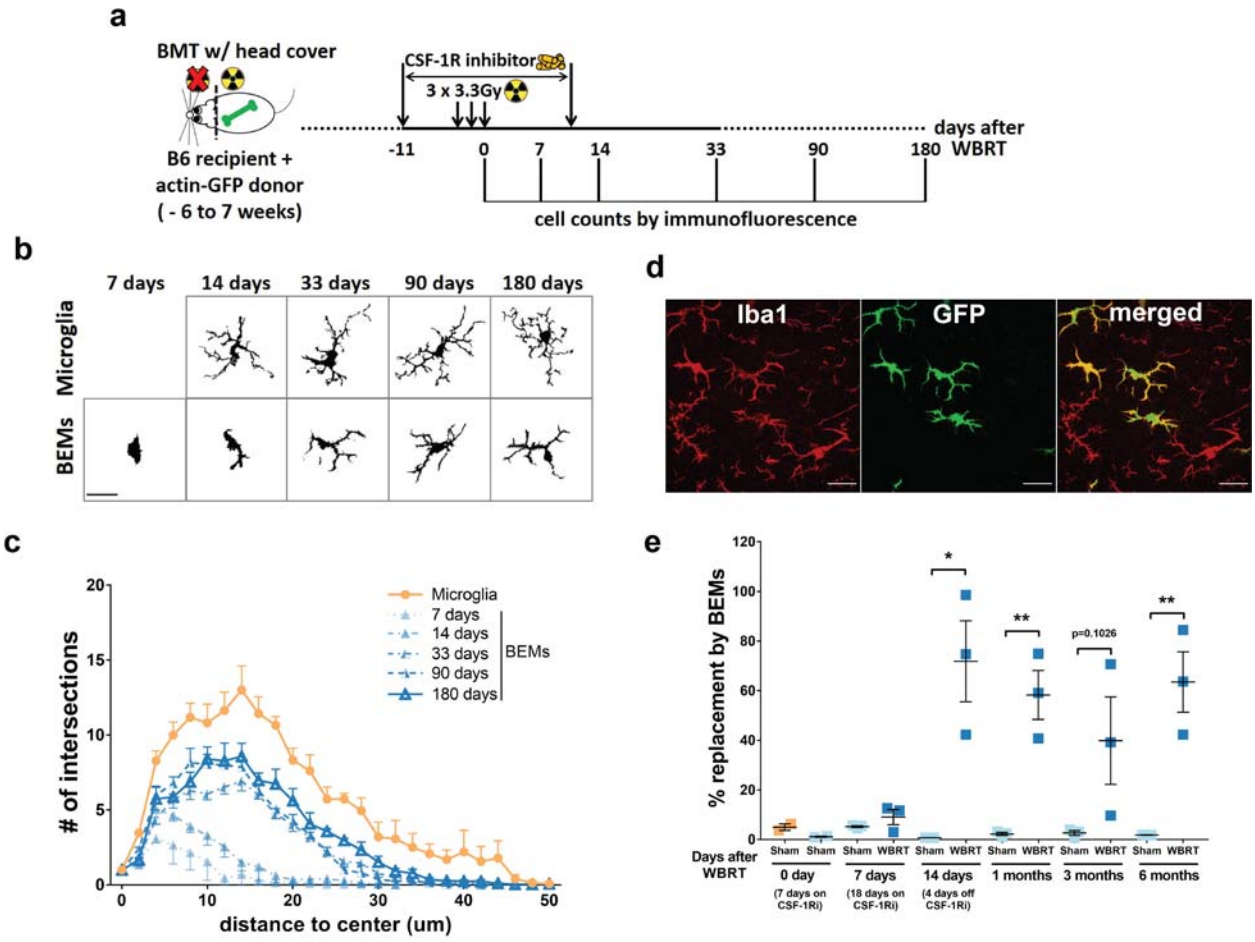
a
BMT w/ head cover
B6 recipient +
actin-GFP donor
(- 6 to 7 weeks)
CSF-1R inhibitor
3 x 3.3Gy
days after WBRT
-11
0
7
14
33
90
180
cell counts by immunofluorescence
b
7 days
14 days
33 days
90 days
180 days
Microglia
BEMs
d
Iba1
GFP
merged
c
Microglia
7 days
14 days
33 days
90 days
180 days
BEMs
# of intersections
distance to center (um)
e
% replacement by BEMs
Days after WBRT
Sham
WBRT
0 day
(7 days on CSF-1Ri)
7 days
(18 days on CSF-1Ri)
14 days
(4 days off CSF-1Ri)
1 months
3 months
6 months
p=0.1026

Figure 3

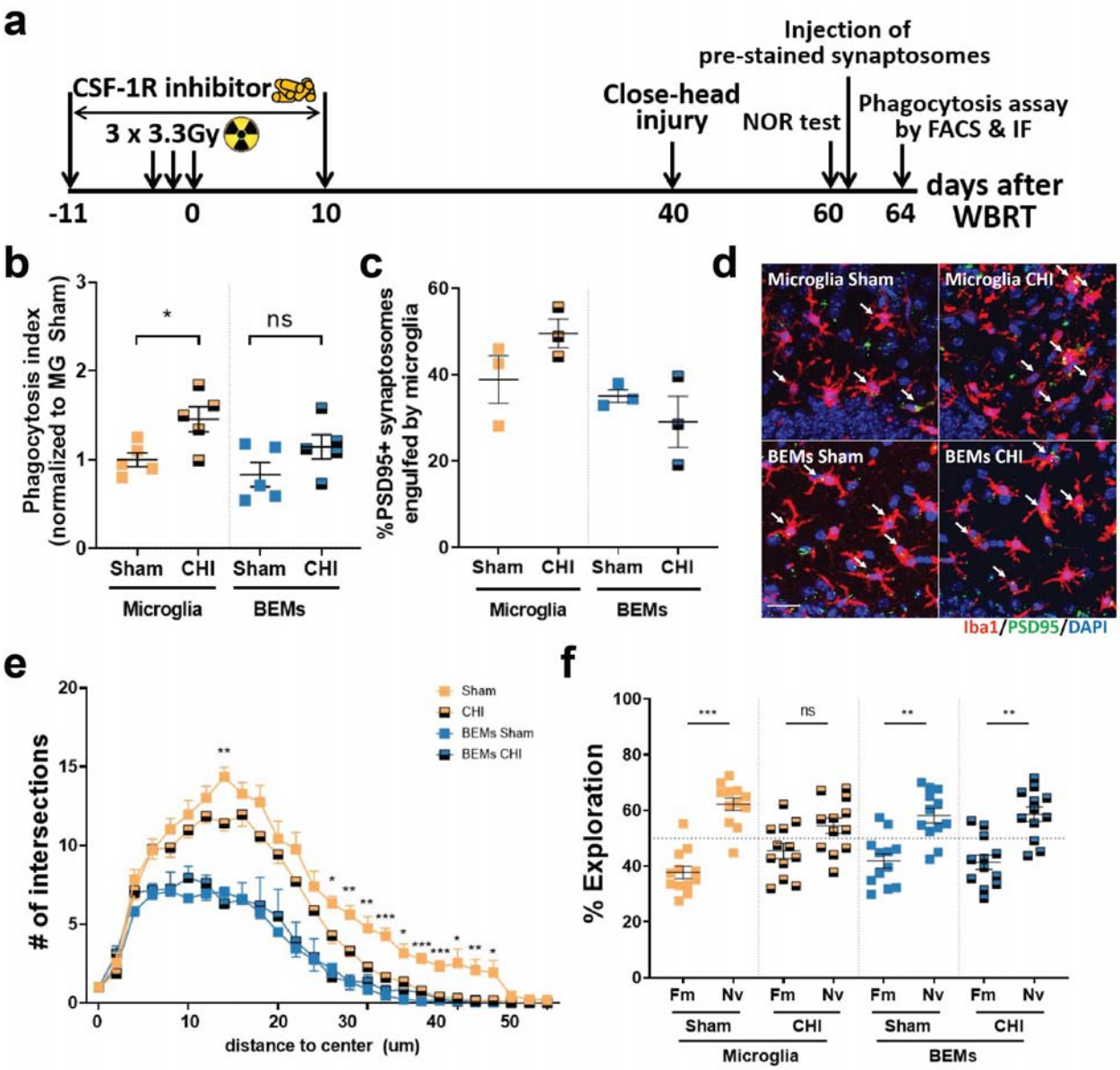
a
CSF-1R inhibitor
3 x 3.3Gy
Injection of pre-stained synaptosomes
Close-head injury
NOR test
Phagocytosis assay by FACS & IF
-11
0
10
40
60
64
days after WBRT
b
Phagocytosis index (normalized to MG Sham)
*
ns
Sham
CHI
Sham
CHI
Microglia
BEMs
c
%PSD95+ synaptosomes engulfed by microglia
Sham
CHI
Sham
CHI
Microglia
BEMs
d
Microglia Sham
Microglia CHI
BEMs Sham
BEMs CHI
Iba1/PSD95/DAPI
e
# of intersections
distance to center (um)
Sham
CHI
BEMs Sham
BEMs CHI
f
% Exploration
Fm
Nv
Sham
CHI
Microglia
BEMs